



## ORIGINAL PAPER

## CONSTRAINING OF STRAIN ELLIPSOID SHAPE FROM SECTIONAL DATA IN THE AU BEARING SHEAR ZONE WEST OF IRAN

Mahdi BEHYARI\* and Afshin KANABI

Department of Geology, Faculty of Sciences, Urmia University, 5756151818, Urmia, Iran

\*Corresponding author's e-mail: [m.behyari@urmia.ac.ir](mailto:m.behyari@urmia.ac.ir)

## ARTICLE INFO

## Article history:

Received 31 October 2018

Accepted 11 February 2019

Available online 21 February 2019

## Keywords:

Ductile shear zone

Strain ellipsoid

Orogenic gold

Flinn diagram

Zagros

Iran

## ABSTRACT

Ductile shear zone recorded valuable data about the progressive deformation and geodynamic setting of the earth crust. Analysis of the strain ratio on the deformed quartz grains in the samples of the Zagros orogenic shear zone indicated generally most of the strain ellipsoids shape are prolate and developed under constructional strain regime. Principal axes of the strain ellipticity ratio varied in the range between 2.04 to 3.12, shear strain magnitude analysis indicated  $\epsilon_s$  are between 0.6 to 1.3. Strain ellipsoid shape also revealed the propagation of the shear zone could not be coeval with the continental collision because in the collision region expected the ellipsoid shape to be oblate. Flattening strain regime in the Zagros Orogeny contemporaneous with the collisional event (D1 phase) and widespread in the Sanandaj-Sirjan Metamorphic Zone. Constructional conditions and prolate strain ellipsoid could be related to the post-collisional deformation phase (D2 phase). In this event stretching and shearing localized in the ductile shear zone and transtension structures superimposed on the former transpression structures. The deformation followed by third phase and brittle event (D3 phase) and caused to the propagation of veins. These veins somewhere cut the foliation and in the other place are parallel to foliation plane.

## 1. INTRODUCTION

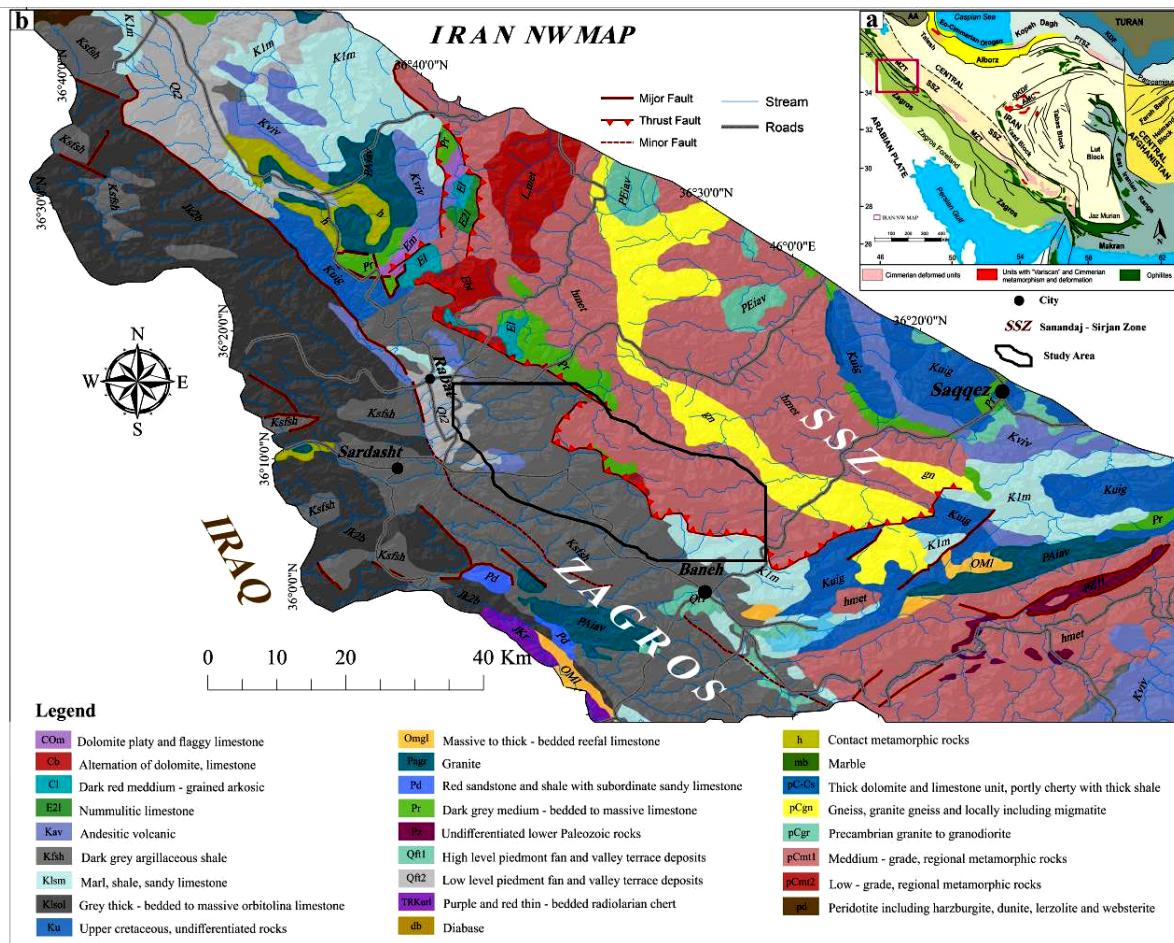
Ductile Shear zones are the widespread structure that localized strain and accommodate deformation in the lithosphere (Ramsay and Graham, 1970; Ramsay, 1980; Simpson, 1981; Shan, 2008; Fossen and Cavalcante, 2017). These zones provide valuable data about the progressive deformation history, such as mineral assemblage and microstructures, P-T conditions and shear sense indicator. These data critically needed to improve understanding of regional tectonics (Watts and Williams, 1983; Zhang et al., 2010; Toy et al., 2012; Mookerjee and Fortescue, 2016).

Primitive research in ductile shear zone proposed that the heterogeneous simple shear is a dominate deformation regime (Ramsay, 1980; Ramsay and Allison, 1979; Ramsay and Graham, 1970; Simpson, 1981; Watts and Williams, 1983) but recent research indicates that in most of the shear zones involve three-dimensional combinations of simple and pure shear strain, such as transpression and transtension zone (Bhattacharyya and Hudleston, 2001; Montési, 2013; Liang et al., 2015; Fossen and Cavalcante, 2017; Behyari and Moghadam, 2018).

Mylonitic rocks formed as a result of heterogeneous shear strain in the ductile shear zone,

and their fabric directly related to the strain rate, finite strain ellipsoid shape and orientation (Watts and Williams, 1983; Zhang et al., 2010; Mulchrone and Talbot, 2014; Fossen and Cavalcante, 2017). Strain ellipsoid shape is an effective tool to the deciphering rheological characteristic and reconstructing progressive ductile deformation history. Therefore in the recent decades, many efforts have been conducted to gain three-dimensional strain ellipsoid shape (Flinn, 1962; Shan, 2008; Mookerjee and Nickleach, 2011; Mulchrone and Talbot, 2014; Soares and Dias, 2015; Mookerjee and Fortescue, 2016).

In the west of Iran recognized shear zone, accommodated mylonite zone that related to the closure of Neo-Tethys and Zagros orogeny contractional event (Mohajjel and Fergusson, 2000; Agard et al., 2005; Allen and Armstrong, 2008; Agard et al., 2011; Mouthereau et al., 2012). Deformation in these shear zones is associated with chemical and mineralogical changes (Aliyari et al., 2009). The circulations of the magmatic fluids convert this zone to be a host for mineralization and ore deposit. The orogenic gold deposit is the typical manifestation in the Zagros collisional Orogenic belt (Aliyari et al., 2009; Alizadeh-Dinabad et al., 2013; Almasi et al., 2015; Almasi et al., 2017). The crustal shear zone has



**Fig. 1** Geological map of the study area. a) Structural map of Iran and tectonic plates and effective faults in the formation of the Sanandaj-Sirjan shear zone and its setting in the regional geodynamic. Red Square showed studied Shear zone in Figure 1b. b) Geological map and access routes to the study area, which has been studied on a smaller scale. It also shows faults and tectonic units. The black area shows the shear zone location in the study.

been playing an important role in the localization strain and providing the proper area for mineral deposition (Heidari et al., 2006; Alizadeh-Dinabad et al., 2013). Nevertheless, the kinematic evolution of deformation in the ductile shear zone, as well as P-T conditions, is not well known. For this reason, spatial and temporal relationship between the episode of ductile deformation and geodynamic evolution, it is not limpid.

In this research, we focused on the kinematic evolution of the ore-bearing ductile shear zone in the Zagros Orogeny and applied strain ellipsoid shape as a vector to the interpretation of structure and intensity of deformation. The main aim is graphically represent the relative principle strain ellipticity ratio on the Flinn diagram and interpret structure developed underwent this deformation conditions. Finally, these data used for the reorganization of structural pattern that controls the strain ellipticity ratio and shape on the orogenic shear zone.

## 2. TECTONIC SETTING AND REGIONAL GEOLOGY OF STUDY AREA

The study area is a part of Zagros Orogeny and located in the Sanandaj-Sirjan metamorphic Zone (SSMZ). The Zagros Mountains in Iran is a part of the Alpine-Himalayan Orogenic belt with the northwest-southeast trending (Fig. 1a). As a result of a northeast-dipping subduction process of the Neo-Tethys oceanic crust, beneath the Iranian micro-continent active margin, formed two major parallel domains with the Zagros suture zone, first is Sanandaj-Sirjan metamorphic Zone (SSMZ) and second is Urumieh-Dokhtar Magmatic Arc (UDMA) (Berberian and King, 1981; Mohajjel and Fergusson, 2000; Agard et al., 2005; Allen and Armstrong, 2008). The subduction process initiated in the late Jurassic (Alavi, 1994; Mohajjel et al., 2003; Ghasemi and Talbot, 2006; Agard et al., 2011) and was terminated by the continental collision between the Arabian and Iranian micro-continent. The timing of the final Neo-Tethys ocean closure and the structure is formed in this tectonic regime is one of the most controversial

subjects. Early contribution emphasized final colliding occurred in the late Cretaceous (Şengör and Kidd, 1979; Berberian and King, 1981; Alavi, 1991; Alavi, 1994), but most of the recent researches assumed closure of Neo-Tethys happened in the Cenozoic (Mohajjel et al., 2003; Agard et al., 2005; Agard et al., 2011; Mouthereau et al., 2012; François et al., 2014). After collision subsequent convergent accommodated along the major thrust and strike-slip fault system and propagated transpression and transtension basin (Jackson, 1992; Mohajjel and Fergusson, 2000; Talebian and Jackson, 2002; Mohajjel and Rasouli, 2014).

In the study area, rock units consist of metamorphosed sequence from the Precambrian to the Tertiary (comprises: Genesis, schist, Mica-schist, and meta-rhyolite). Mesozoic rocks in the study area deposited after a long interval with older units; this contains a complex of volcanic-sedimentary. These units have widespread exposure, high thickness and metamorphosed to greenschist facies (Aliyari et al., 2009; Alizadeh-Dinabad et al., 2013; Almasi et al., 2015; Almasi et al., 2017) (Fig. 1b).

The Eocene volcanic unit is the youngest non-metamorphic volcanic activity in the study area. The transpression tectonics regime is dominated in the Cenozoic and particularly in the Eocene (Mohajjel and Fergusson, 2000), and could be facilitated volcanic activity (Fig. 1b).

Consideration to the regional map (Fig. 1b) revealed the study area located in the transition zone between Zagros sedimentary basin and SSMZ, indeed this area coincides with the suture zone between the Arabian plate and Iran micro-continent. Ophiolite mélange in the Baneh area with NW-SE trend continued to the west over the border of Iraq. This unit is tectonically mélange and is impossible to be recognized sedimentary units from ultramafic segments. The sedimentary part includes 20 percent of the whole of ophiolite mélange volume. This part includes two different facieses: pelagic limestone with the Paleocene age and grey limestone of the Eocene age (GSI, 1976). The boundary sedimentary units with ultra-mafic units is a thrust fault, the dip of the fault plane is towards N-NE (Agard et al., 2005).

In the southern part of the study area, Eocene deposits were affected by several faults so that in some parts, they mixed with the ophiolite.

### 3. STRUCTURAL ELEMENTS

Deformation and metamorphism in the convergent plate boundary caused to superimposition of the different phases of deformation and propagated the complex structural pattern. In the study area collisional event of the Neo-Tethys followed by the magmatic body intrusion (Azizi et al., 2018; Zhang et al., 2018; Behyari et al., 2018) and development of complex structures, consists of: foliation, ductile shear zone, and brittle structures such as conjugated fault, fractures and veins. The deformation history of study area can be classified into three stage. The first stage

is a co-axial penetrative deformation that affected Paleozoic units and developed pervasive foliation. The second events are non-coaxial and non-penetrative deformation concentrated in the shear zone. In the some parts of the study area this deformation phase overprint on the older deformation phase. The main structures propagated in this phase are mylonitic and S-C fabric, Minerals fish and lensoid structures, and shear folds. The third deformation phase is the semi-brittle phase and fractures and brittle faults are the results of this phase. In this section, the structures describe according to the precedence of evolution and investigated variation of strain ellipticity ratio and shape in the collisional zone:

#### 3.1. D1 DYNAMO-THERMAL REGIONAL DEFORMATION:

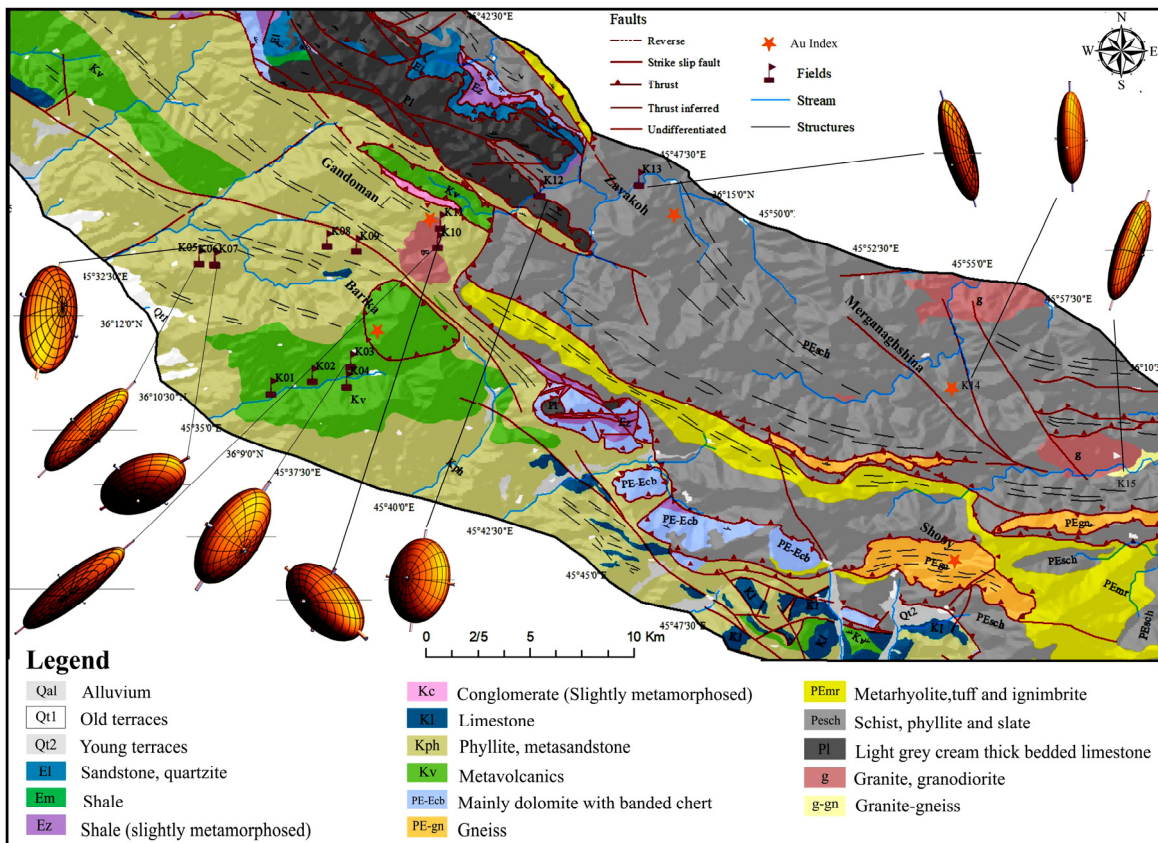
This phase of deformation occurred contemporaneously with the regional metamorphism in the SSMZ. The foliation is the most important structure developed in this stage (Sarkarinejad et al., 2010; Sheikholeslami, 2015). The deformed Precambrian unit consists of schist, phyllite, and slate, exposed extensively in the east and south-east of the study area. The ribbon of meta-Rhyolite, metamorphosed acidic tuff and ignimbrite lie parallel to this Precambrian unit (Fig. 2).

The foliation general spatial orientation is parallel to the main thrust fault in the study area and the Zagros faults strike NW-SE in this region (Agard et al., 2011; Mohajjel and Fergusson, 2000). In the K03 station near the Barika Au-index foliation planes, attitude is N40°W/50°NE, these foliated planes superimposed by subsequent deformation path. Around this area in K04 and K05 foliation, attitude is approximately same to the K01 station (Fig. 2).

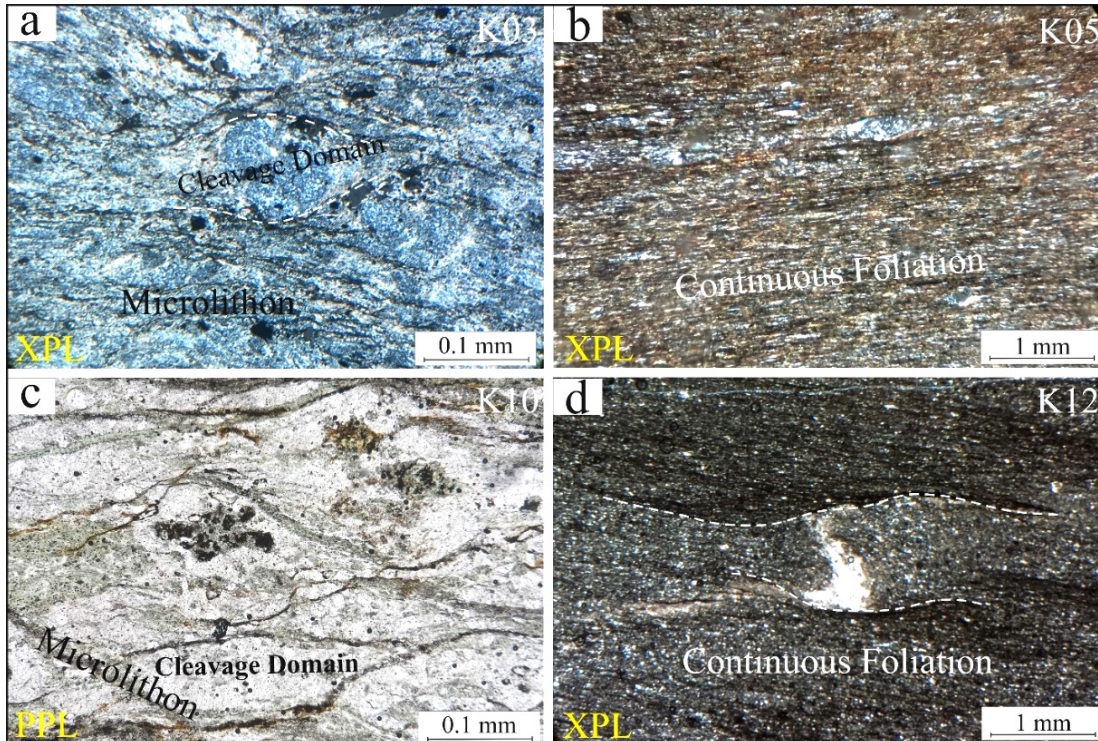
In the Gandoman Au-index (K06, K07), two foliation planes propagated, and the dominant foliation is parallel to the previous stations, but the dip of the plane increased respect to the Barika index (K01, K04). On average these set of the foliation plane's attitude are N30°W/70°NE. The weaker foliation set trend is NE-SW and has dipped to the NW, the measurement of this set of foliation indicated general orientation is N20°E/50°NW. In the other Au-indexes such as Zavakoh (K13), Merganagshina (K14), Shooy (K15) foliation general trend is NW-SE and dip direction is toward NE and dip of foliation plane change in the wide range between 30° to 70°.

In the thin section used XZ and YZ planes data for the explanation of foliation morphology. In the K03 propagated spaced foliation. Cleavage domain contains opaque mineral and microlithons are consist of very fine grain of plagioclases. A weak crenulation developed in the cleavage domain, but it is not penetrative in the section. This crenulation in somewhere caused to the propagation of new foliated plane. The shape of the cleavage domain is smooth and spatial relation between cleavage domains is anastomosing (Fig. 3a).



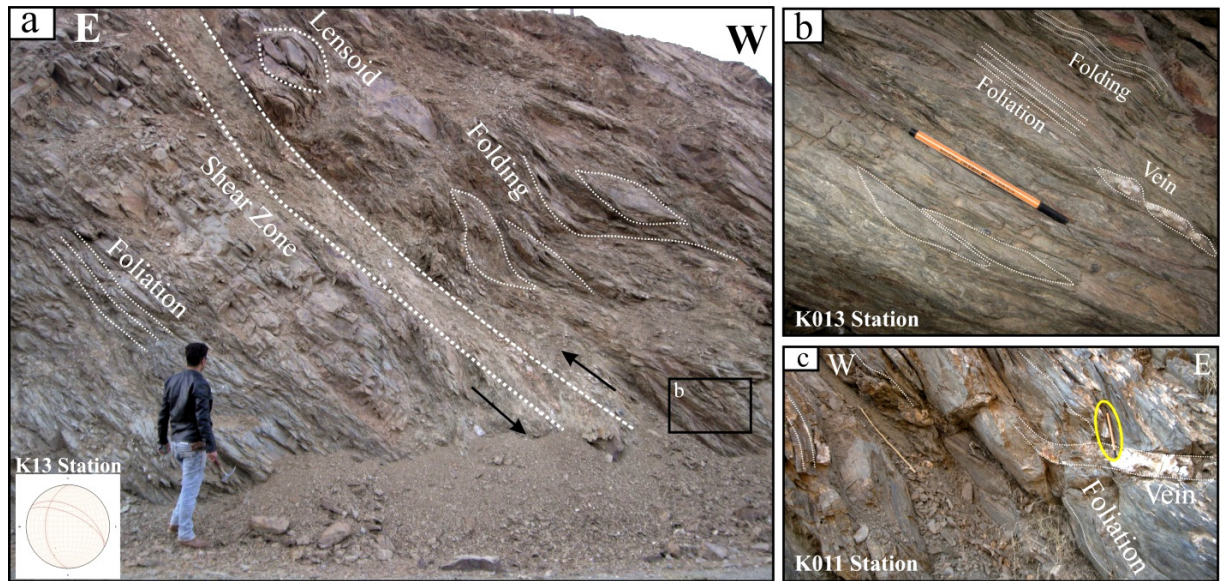


**Fig. 2** Structural map of the shear zones and faults in the study region. It also shows Au-index, and three-dimensional ellipsoid strain shape.



**Fig. 3** Microscopic studies and thin section analysis of foliation morphology that developed in D1 Deformation phase, a) spaced foliation in K03 station. Cleavage domain contains opaque mineral and microlithons very fine grain plagioclases. b) Continuous foliation propagation in the phyllite units. The volume percentage of cleavage domain is above 90 % and quartz filled veins cut the foliation plane. c) In the Metavolcanics units (K10) weak spaced foliation propagated. The cleavage domain contains fine grain sericite and microlithones consist of deformed quartz. d) The foliation type in Precambrian Schist, phyllite and slate units (K12) is fine grain and continuous. These foliation plane penetrated in the whole of the rock volume.





**Fig. 4** Field photographs. a) lensoid shape and folded foliation in the K13 shear zone. black box show the location of Figure b. b) The quartz vein injected parallel to the foliation plane and boudin underwent of shear stress. Propagation of folding and sigmoid structures can be seen in shear zone. c) quartz vein in the shear zone cut the foliation plane.

The foliation type in the Phyllite, meta-sandstone unit (K05) is continuous and very fine grain, fabric elements are homogeneously distributed in the rock. The volume percentage of cleavage domain is above 90 % and quartz filled veins cut the foliation plane (Fig. 3b). In the Meta-volcanic rocks (K10) weak spaced foliation propagated. The cleavage domain contains fine grain sericite and microlithones deformed quartz (Fig. 3c). The foliation type in Precambrian Schist, phyllite and slate units (K12) is fine grain and continuous. These foliation planes penetrated in the whole of the rock volume (Fig. 3d). In the other samples from this unit (K13, K14, K15) the strong superimposition of subsequent deformation phase removed evidence of the D1 foliation. Generally this stage of deformation affected Paleozoic and Mesozoic rock units also with attention to the pervasive effect of D1 event in the SSMZ, assumed this phase occurred contemporaneously with the collision of Arbain plate with the Iranian micro-continent.

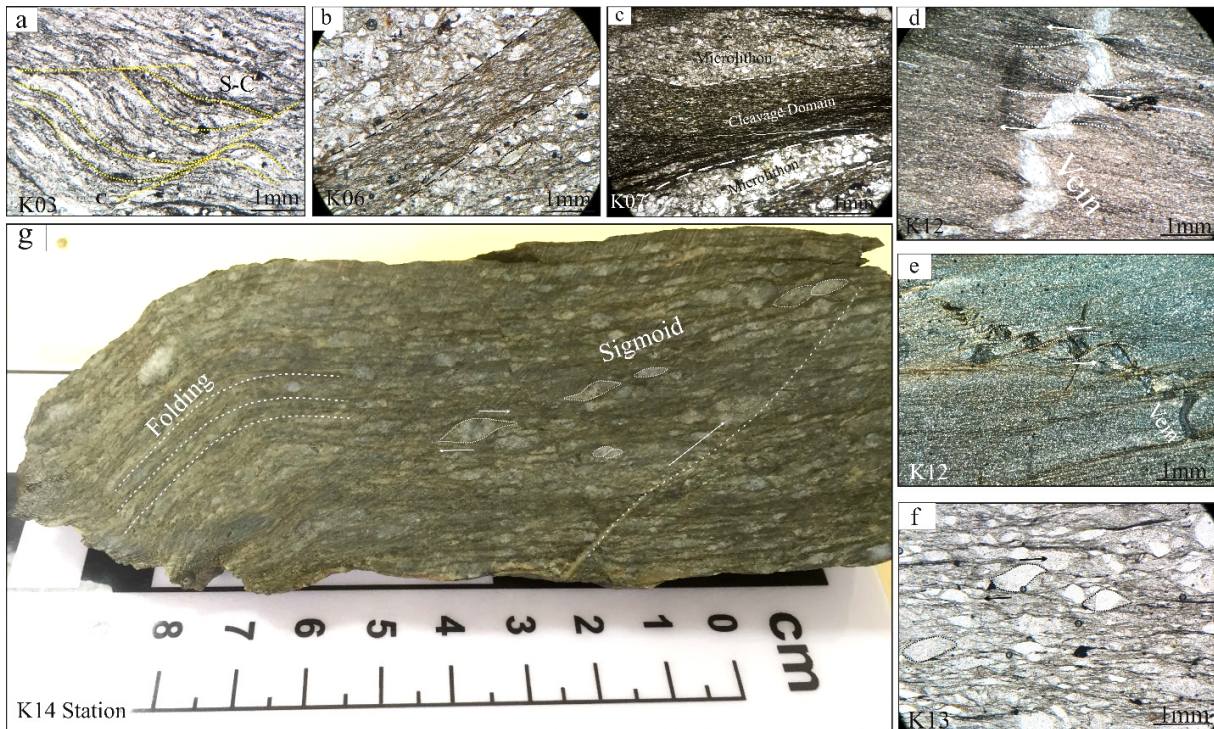
### 3.2. D2 DUCTILE-SHEAR DEFORMATION:

The dynamo-thermal regional deformation followed by severe ductile deformation. This phase is the most important event in the study area and associated with the development of the high strain, Au-bearing ductile shear zone (Aliyari et al., 2009; Almasi et al., 2017). Event D2 is related to the post-collisional contraction in the Zagros suture zone. Deformation evidence of this phase mostly has been studied in the ductile shear zone. The mylonitization is one of the significant effects of ductile deformation in this period and propagated mylonitic foliation with the NW-SE general trend.

The shear zone spatial orientation measured in the different station, in average N60W/50NE, is the shear zone orientation, this trend is approximately parallel with the Zagros Orogeny (Fig. 4a). In the ductile shear zone outcrop, the frequent deformed structures are the folded mylonitic foliation and well developed S-C structure. S-plane and C-plane combined with each other and created lensoid shape structures in the rock units (Fig. 4b). Also folded and sheared silica vein is the common structure in the shear zone. These veins are in two sets, first set cut the foliation and second are parallel to the foliation plane (Fig. 4c).

The thin section feature has been used for determination of sense of shear, the intensity of deformation, P-T condition in the shear zone and deciphering strain ellipsoid shape. Thirty thin sections from ten samples covering all the deformation event in this phase. At the K03 station in the XZ plane dominant structures are distinct light and dark bands that are typical of in the ultra-mylonite. The striped mylonite structure consists of continuous bands of mostly recrystallized grains, this plane attitude is N40°W/60°NE approximately parallel to the foliation and connected with the shear plane. These structures proposed sinistral shear sense for this zone (Fig. 5a). In the K06 recrystallized fabric with frequent porphyroclasts revealed earlier mylonitization stage. Relict quartz porphyroclasts underwent ductile deformation indicate sweeping and undulatory extinction. Also fabric elements in the result of shear strain showing preferred orientation. Cleavage domain composed of dark biotite, opaque minerals, and a few hornblende and microlithon contains light long and lozenge-shaped relict quartz grains. The width of dark





**Fig. 5** Microscopic and hand sample evidence of shear in the study area, a) the folding and foliation of the S-C fabric structures are shown at the Barika Au-Index station (K03). b, c) At stations K06 and K07, minerals have been elongated and propagation of microlithon and cleavage-domain. d, e) These two Figures indicated the penetration of quartz veins that have been sheared due to the displacement along the foliated plane. f) The microscopic section is related to the shear zone of the K13 station, the minerals completely elongated and formed sigmoid structures. g) The hand sample from station K14, with sigmoid structures and folding and foliation.

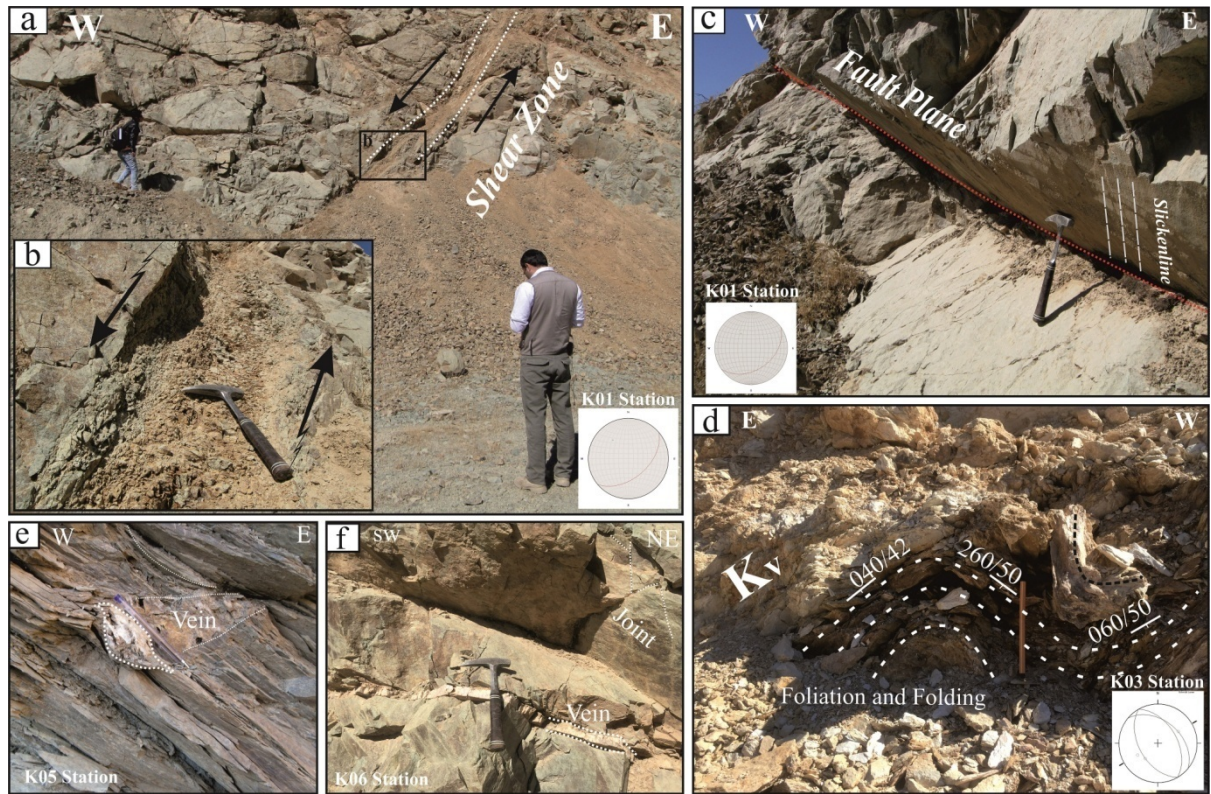
and light zone increased in this sample (Fig. 5b). In the K07 station grains indicated more evidence of strain than the K06 station, proposed that the deformation was accommodated by recrystallization and grain size reduction. In the cleavage domain increased the concentration of dark grains and in the microlithone decreased prophyroclast size and frequency (Fig. 5c). At the other stations and samples, the structure elements are similar to the described stations, mylonitic foliation and shear structure are dominated and attitude of structures is approximately identical. The deformed basement in the study area comprises of Precambrian schist, phyllite, slate, and cut by Au-bearing ductile shear zone samples K12, K13, K14 are from these shear zones. The main change in K12 respect to the other station is the propagation of continuous foliation accompanied by notable grain size reduction. The veins cut the foliation plane and showed sinistral displacement along the shear plane (Fig. 5d). One of the Au-bearing shear zones is the Zavekouh shear zone in the east of the study area. The sample K13 is quartzite mylonite (medium grade mylonite) and taken from this shear zone. The main difference with respect to other shear zones in the study area is well-developed quartz porphyroclast texture accompanied by dextral sheared microstructure and preferred orientation. The quartz

mineral fish widely propagated and indicated dextral shear component also long and lozenge shape quartz microstructures are immersed in a very fine-grained matrix (Fig. 5f). Mylonitic foliation is a penetrative structure in the shear zone. Deformation mechanism in the K14 (Merganagshina) station is similar to the K13. The quartz porphyroclasts showing dextral shear and mostly have preferred orientation. With attention to the commonly used classification of mylonites is based on the percentage of matrix respect to the porphyroclast) this shear zone is medium grade mylonite (Passchier and Trouw, 2005). In the hand sample folding of the foliated plane is emerged (Fig. 5g). Quartz grains, mostly have sigmoid shape. The striped structure propagated by the sequence of dark and light grains arranged in the approximately mono-minerals layers.

### 3.3. D3 LOW-TEMPERATURE BRITTLE EVENT:

The latest deformation path in the study region is a low-temperature brittle deformation phase acted after ductile deformation and mylonitization processes. This retrograde deformation phase characterized by the faults, micro-fracture which cut through the foliation propagated during ductile events. Micro-fracture, mostly filled with quartz grains and caused to the propagation of silicification and sulfide



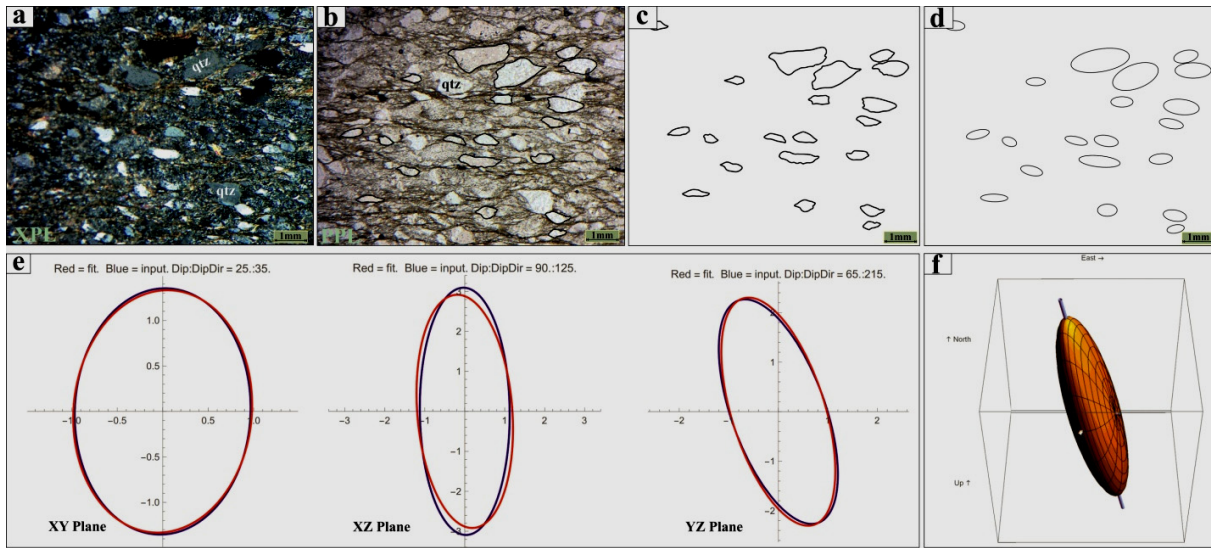


**Fig. 6** Field photographs. a) Brittle fault zone in the K01 station and concentration of fracture in this area (Black square is showed location of Figure 6b). b) in-cohesive fault breccia in the K01 station, c) The fault plane and slickenline in the thrust fault. d) Foliation and folding of thick layer in the Barika Au-Index in the K03 station. e) The calcite fill vein parallel to the foliation plane.

alteration. Geochemical analysis revealed these zones coincident with the concentration of Au in the ore-bearing shear zone (Aliyari et al., 2009). Several types of faults with the various attitude developed during this brittle events. Fault zone characterized by the concentration of fracture and fault breccia. Conjugated faults also are one of the common structures in this brittle zone, the general trends of faults are NE-SW and NW-SE (Fig. 6a). Brecciated zone width with tens of centimeters is most common (Fig. 6b). Precambrian recrystallized deformed basements exhumed along the thrust faults in some outcrops thrust fault plane preserved, field data revealed these type faults, general attitude is N45°E/40°SE and slickenlines spatial orientation are 185°/80° and have dextral strike-slip component (Fig. 6c). In the fault zone under compressional conditions propagated folded layers (Fig. 6d). Fracture in the fault zone, mostly filled with the quartz and calcite, these veins can be divided into two categories based on the orientation of the vein with respect to the foliation plane. The first set is cut through the foliation plane, these veins are more abundant and have a less aperture than other veins (Fig. 6e). The second set of veins inject along the foliation plane and are parallel to these surfaces. These veins are mostly thick and filled with calcite (Fig. 6f).

#### 4. METHODOLOGY

For calculating the strain ellipsoid shape in the ore-bearing shear zone in the study area, applied a suite of the geological program developed by (Mookerjee and Nickleach, 2011) and written in the Mathematica. The advantage of this program is utilized of arbitrary sectional ellipses to determining a general ellipsoid. The sample preparation process conducted according to the (Mookerjee and Fortescue, 2016), for this purpose 10 samples collected along the ore-bearing shear zone in the study area. Thin section for microscopic study prepared in three perpendicular directions. XY section indeed is foliation plane and XZ section are perpendicular to XY section and foliation plane strike, finally YZ section are perpendicular to the both of XY and XZ section. In the next step with attention to the lithology units of the study area selected quartz grain as strain index. Photomicrographs were taken and merged with each other to gain complete thin section image (Fig. 7a). Graphical program effects applied to the edge enhancement of quartz grain, then selected grain boundary to down on the photomicrographs (Fig. 7b), in each thin section between 50 to 100 grains used to refine strain estimation. This drawing figures exported as an individual layer to the ImageJ program (Fig. 7c). This program used to trace the best fit ellipse for imported quartz grains (Fig. 7d). The resulted dataset



**Fig. 7** The steps of the extracting three-dimensional strain analysis method are shown respectively. a) Example selected thin section under XPL light. b) Digitally tracked quartz grains in bridge light after edge enhancement. c) The exported individual image, which should be white for more precision. d) The resulting, ImageJ-determine, best-fit ellipse for each tracked grain. e) The Mathematica output of the mean sectional ellipse with respect to the best-fit ellipse for a given section. f) The resulting three-dimensional strain was drawn for the sample.

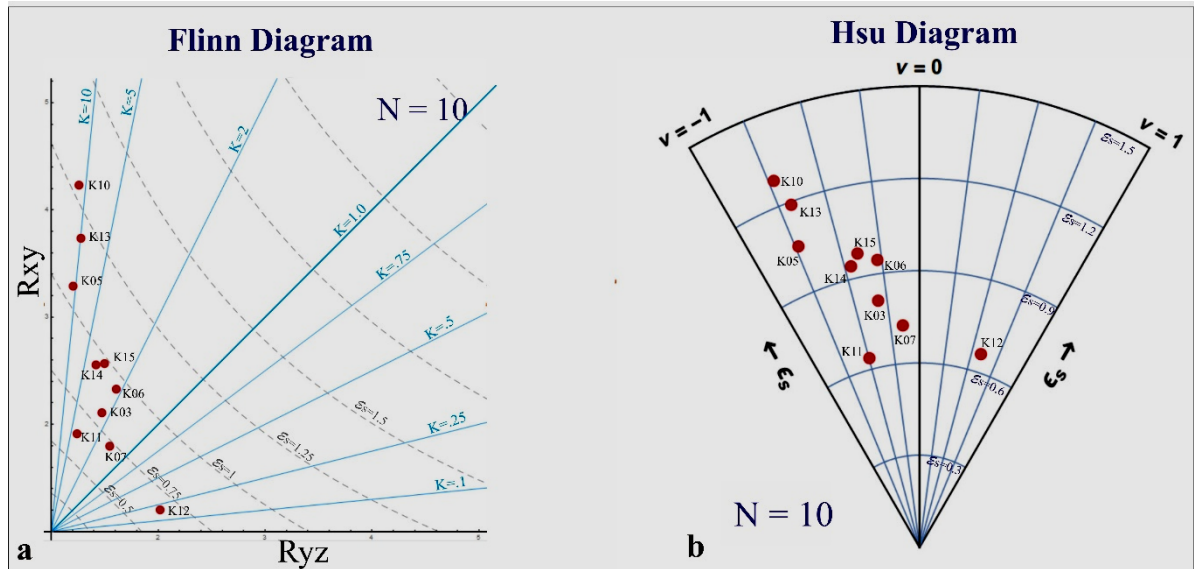
exported as Microsoft office Excel datasheet. This dataset imported to the Mathematica script, “Best-Fit Ellipsoid with Statistics for ImageJ with Vort-v3\_0.nb” (Mookerjee and Nickleach, 2011). This process conducted for elliptical quartz marker in the three XY, XZ and YZ section (Fig. 7e). Finally best fit ellipsoid extracted with each of sectional planes (Fig. 7f).

## 5. DISCUSSION:

Complicated deformation history in the study area is related to the geodynamic setting of this region and collisional event in the Zagros orogeny (Agard et al., 2011; Mohajjel and Fergusson, 2000; Mouthereau et al., 2012). This collision event coincident with regional deformation in green-schist facies in the SSMZ. After collision contractions in the suture zone accommodate by transpression shear zone (Mohajjel and Rasouli, 2014). These shear zones in the earth crust provide a high permeability fractured zone, and facilitated the circulation of hydrothermal fluid that mostly accompanied with the mineralization. High concentration of Au in the ductile shear zone directly related to the deformation intensity in the study area (Aliyari et al., 2009; Alizadeh-Dinabad et al., 2013; Almasi et al., 2015; Almasi et al., 2017). Strain ellipsoid geometry provides important data about deformation history in the shear zone (Mookerjee and Nickleach, 2011). The perfectly oblate strain ellipsoid is common in the shear zone that deformed underwent flattening strain and perfectly prolate ellipsoid developed under constructional strain regime (Fossen and Cavalcante, 2017; Mookerjee and Peek, 2014). To gain strain ellipsoid shape requested the axial ratio of

the long and intermediate ( $R_{xy}$ ) and intermediate and short axes ( $R_{yz}$ ). These data extracted from the deformed quartz shape on the XY and YZ thin section for each sample also shear strain are proportional with  $R_{xz}$  therefore, this value also calculated for each sample. Strain ellipsoid principal axes ratio increasing, accompanied with increasing of deformation intensity. In the study area high deformed zone characterized by grain size reduction and recrystallization of protolithic grain, relict porphyroclast frequency decreased and finally increased foliation volume percentage respect to the whole of the rock unit. Evaluating of calculating  $R_{xz}$  in the samples indicated the value varied between 2.45 to 4.25 and total strain ellipsoid principal axes ratio range is between 2.04 to 3.12. Strain ellipsoid shape in all stations except K12 is prolate and formed under constructional strain conditions. In the K12 strain ellipsoid shape is oblate and propagated in the flattening regime. This interpretation has the important geodynamic concept. In the collision zone expected oblate strain ellipsoid shape and dominant deformation mechanism be flattening. This data revealed Au-bearing ductile shear zone cannot be coeval with the collisional event (D1 deformation phase). After the closure of Neo-Tethys and continental collision contraction in the suture zone accommodate by propagation of ductile shear zones. In this period Urmia-Dokhtar magmatic arc was active in the study area and magmatic fluid penetrated in the ductile shear zones and deposit the Au mineral. Constructional strain in the shear zones caused to developed sheared and stretched structure. Indeed post-collisional (D2 phase) transtension evidence





**Fig. 8** Geometric data is a three-dimensional strain for 10 samples, resulting in 9 samples are in a prolate shape and only 1 sample is oblate. a) Flinn diagram and b) Hsu diagram.

superimposed on collisional (D1 phase) transpression structure in the Zagros collision zone. The evidence of this superimposition of transtension on transpression in the brittle shear zone well documented by (Mohajjel and Rasouli, 2014). The strain ellipsoid parameters and shear intensity varied in the different samples and stations. In the K03 station (Barika Au-index),  $R_{xy}=1.29$  and  $R_{yz}=2.43$  and the total finite strain ratio equal to 2.05, the foliated plane (XY plane) developed on the D1 phase superimposed by stretching lineation in D2. K05 station is located near the high strain ductile shear zone with NW-SE trend.  $R_{xy}=1.31$  and  $R_{yz}=3.82$  and total final strain ratio are 3.12. Strain ratio in the XZ plane equal to  $R_{xz}=4.22$  and imply to high shear strain in this station. This strain condition caused to propagation ultra-mylonite unit and increased foliation percentage to the rock volume intersection of the foliated plane and stretching lineation increased the permeability of the zone. K06 and K07 located near the K05 station on the Phyllite, metasandstone unit the common characterize of these stations is the relatively high value of strain ellipsoid principal axes ratio on the XZ plane. Gandoman Au-bearing ductile shear zone strain ellipsoid studied by samples K10 and K11. In the K10 total strain ellipsoid principle axes ratio is 2.04 and in K11 is 2.21.  $R_{xz}$  also calculated on the XZ plane for K10=2.65 and K11=2.93. The K12 is a spatial sample, because in this station strain ellipsoid shape is different with other station. This sample taken from a thrust fault zone and contraction of fault zone caused developed the oblate shape of strain ellipsoid. Mean principal axes orientations calculated for all stations and projected in the lower hemisphere, equal-area stereonet. This data indicated wide range, diversity for long, intermediate and short axes orientation. The rotation of the principal strain axes is related to high

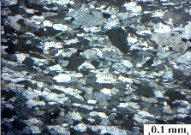
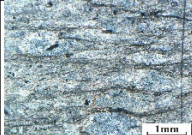
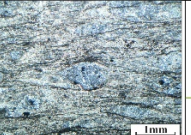
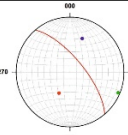
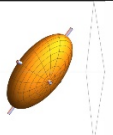
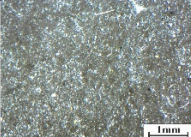
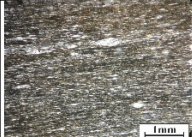
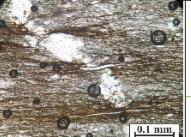
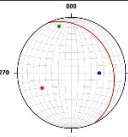
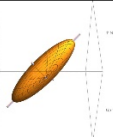
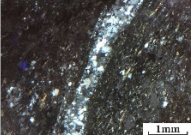
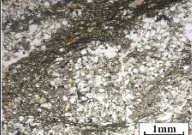
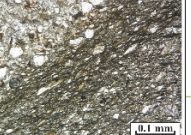
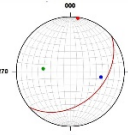
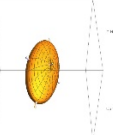
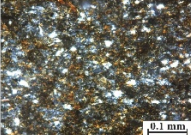
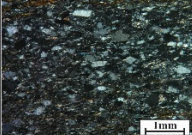
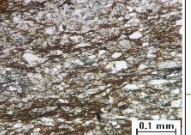
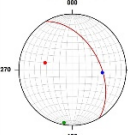
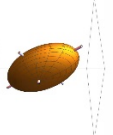
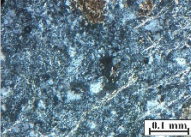
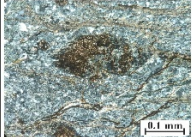
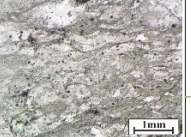
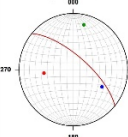
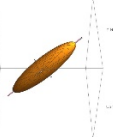

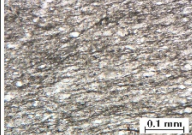
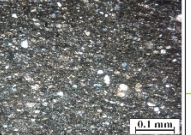
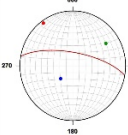
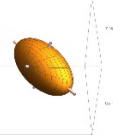
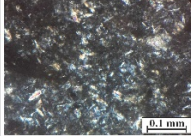
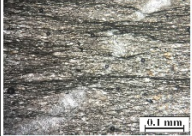
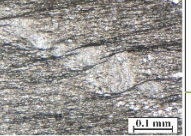
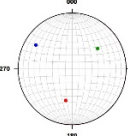
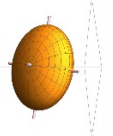
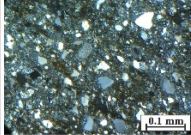
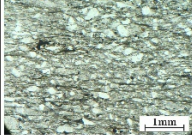
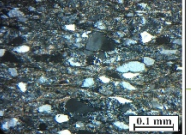
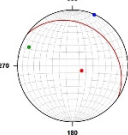
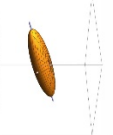
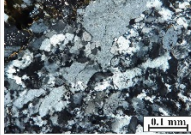
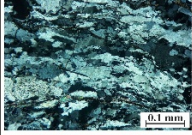
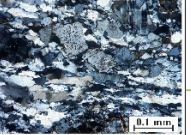
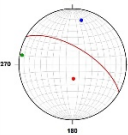
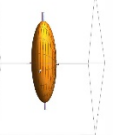
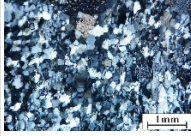
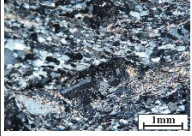
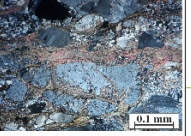
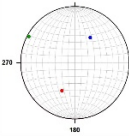
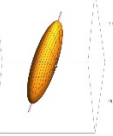
vorticity during the progressive deformation in the shear zone. Approximate estimation imply the general orientation of strain ellipsoid long principal axes is NE-SW and plunge varied between  $30^\circ$  to  $50^\circ$  (Table 1).

For the visualized the strain ellipsoid shape and interpretation data all principle axes measurement in the XY and YZ plotted to the Flinn diagram. Strain ellipsoid geometry in the study area, mostly are prolate and only K12 sample set in the oblate zone (Fig. 8a). Strain magnitude generally increases away from the origin, therefore in K10, K13, K05 occurred maximum stretching (Flinn, 1962; Fossen, 2016). In the Hsu diagram data plotted on the  $60^\circ$  sector of the circle, the lode ratio ( $V$ ) defined the strain ellipsoid shape and shear strain ( $S$ ) represent the intensity of strain in the shear zone (Fig. 8b). This diagram indicated shear strain in most of shear zones in the study area is more than 0.9.

## 6. CONCLUSION:

Structural analysis in the study area revealed a poly-phase deformation that caused to propagate complicate high strain zone accompanied with Au mineralization. The first deformation phase is dynamo-thermal regional event could be coincides with the closure of Neo-Tethys in the Zagros orogeny and propagated a penetrative spaced foliation under the flattening conditions and nearly oblate strain ellipsoid. The second phase followed by the contraction in the suture zone and accommodated by the transpressional ductile shear zone. Stretching in the ductile shear zone under constructional regime caused to propagation the prolate strain ellipsoid shape. The strain axes ratio in the XY and YZ section at high strain ductile shear zone indicated strain ellipsoid shape in the most of the shear zone is prolate

**Table 1** A summary of all station microscopic images (XY, XZ and YZ Plane), R values, strain ellipsoid principal axes ratio, also principal strain axes ratio projected on stereonet. The resuled three-dimensional strain was drawn for the all samples. Approximate estimation implies the general orientation of strain ellipsoid long principal axes is NE-SW and plunge varied between 30° to 50°.

Sample	Thin Section XY Plane	Thin Section XZ Plane	Thin Section YZ Plane	Rxy Rxz Ryz R	Principal Axes Orientation	Strain ellipsoids
K03 558316 m E 4004629 m N				1.290 2.455 2.413 2.052		
K05 552392 m E 4009553 m N				1.310 4.228 3.823 3.120		
K06 552999 m E 4009504 m N				1.382 3.254 2.157 2.264		
K07 552986 m E 4009508 m N				1.371 3.398 2.662 2.477		
K10 561638 m E 4010374 m N				1.373 2.655 2.115 2.047		
K11 561742 m E 4011307 m N				1.615 2.932 2.085 2.210		
K12 565595 m E 4012891 m N				1.270 3.306 2.329 2.301		
K13 569416 m E 4013426 m N				1.401 2.524 2.517 2.147		
K14 582487 m E 4008367 m N				1.494 2.663 2.218 2.125		
K15 588475 m E 4003213 m N				1.711 2.783 2.314 2.269		



and formed under the constructional regime and only in the one station oblate strain ellipsoid propagated under flattening conditions. With increasing deformation in ductile shear zone ascending the Au deposition and evaluating of strain magnitude showed generally in the shear zones of the study area shear strain are more than 0.9 and maximum shear accommodate in the station K10, K13, K05.

The strain ellipsoid shape also indicated propagation of shear zone could not be coeval with the continental collision because the collision region expected the ellipsoid shape to be oblate. Indeed, transpression in the Zagros Orogeny contemporaneous with the collisional event (D1 phase) and widespread in the SSMZ but transtension event is related to post-collisional deformation phase (D2 phase) and localized in the ductile shear zone. The third deformation phase is a brittle event and caused to the propagation of veins. These veins somewhere cut the foliation and in the other place are parallel to foliation planes.

#### ACKNOWLEDGEMENTS:

This project financials support provide by Urmia University. We grateful to research Bureau of Urmia University to the authorities. We also thankful to the Dr. Matty Mookerjee for kindly help to the utilized of Mathematica script.

#### REFERENCES

- Agard, P., Omrani, J., Jolivet, L. and Mouthereau, F.: 2005, Convergence history across Zagros (Iran): constraints from collisional and earlier deformation. *International Journal of Earth Sciences*, 94, 401–419. DOI: 10.1007/s00531-005-0481-4
- Agard, P., Omrani, J., Jolivet, L., Whitechurch, H., Vrielandck, B., Spakman, W., Monie, P., Meyer, B. and Wortel, R.: 2011, Zagros orogeny: a subduction-dominated process. *Geological Magazine*, 148, 692–725. DOI: 10.1017/S001675681100046X
- Alavi, M.: 1991, Sedimentary and structural characteristics of the Paleo-Tethys remnants in northeastern Iran. *The Geological Society of America Bulletin*, 103, 983–992. DOI: 10.1130/0016-7606(1991)103<0983:SASCOT>2.3.CO;2
- Alavi, M.: 1994, Tectonics of the Zagros orogenic belt of Iran: new data and interpretations. *Tectonophysics*, 229, 211–238. DOI: 10.1016/0040-1951(94)90030-2
- Aliyari, F., Rastad, E., Mohajjel, M. and Arehart, G. B.: 2009, Geology and geochemistry of D–O–C isotope systematics of the Qolqoleh gold deposit, Northwestern Iran: Implications for ore genesis. *Ore Geology Reviews*, 36, 306–314. DOI: 10.1016/j.oregeorev.2009.06.003
- Alizadeh-Dinabad, H., Ghavami-Riabi, R., Eslamkish, T. and Mirzaei, Y.: 2013, Controlling factors on changes of gold mineralization in Saqqez (Kurdistan) shear zones and reagent ratios of the mineralized section. *Arabian Journal of Geosciences*, 6, 1457–1464. DOI: 10.1007/s12517-011-0450-0
- Allen, M.B. and Armstrong H.A.: 2008, Arabia-Eurasia collision and the forcing of mid-Cenozoic global cooling. *Palaeogeography, Palaeoclimatology, Palaeoecology*, 265, 52–68. DOI: 10.1016/j.palaeo.2008.04.021
- Almasi, A., Jafarirad, A., Afzal, P. and Rahimi, M.: 2015, Prospecting of gold mineralization in Saqez area (NW Iran) using geochemical, geophysical and geological studies based on multifractal modelling and principal component analysis. *Arabian Journal of Geosciences*, 8, 5935–5947. DOI: 10.1007/s12517-014-1625-2
- Almasi, A., Yousefi, M. and Carranza, E.J.M.: 2017, Prospectivity analysis of orogenic gold deposits in Saqez-Sardasht Goldfield, Zagros Orogen, Iran. *Ore Geology Reviews*, 91, 1066–1080. DOI: 10.1016/j.oregeorev.2017.11.001
- Azizi, H., Hadad, S., Stern, R.J. and Asahara, Y.: 2019, Age, geochemistry, and emplacement of the ~40-Ma Baneh granite–appinite complex in a transpressional tectonic regime, Zagros suture zone, northwest Iran. *International Geology Review*, 61, 2, 195–223. DOI: 10.1080/00206814.2017.1422394
- Behyari, M. and Moghadam, H.H.: 2018, Emplacement of silica veins at a brittle shear zone in the Ahar region, NW Iran: Insights from structural analysis, analogue and numerical modeling. *Journal of African Earth Sciences*, 144, 90–103. DOI: 10.1016/j.jafrearsci.2018.04.011
- Behyari, M., Nouraliee, J. and Ebrahimi, D.: 2018, Structural control on the Salmas geothermal region Northwest Iran, from fractal analysis and paleostress data. *Acta Geologica Sinica*, 92, 5, 1728–1738, (English Edition). DOI: 10.1111/1755-6724.13673
- Berberian, M. and King, G.C.P.: 1981, Towards a paleogeography and tectonic evolution of Iran. *Canadian Journal of Earth Sciences*, 5, 101–117. DOI: 10.1139/e81-019
- Bhattacharyya, P. and Hudleston, P.: 2001, Strain in ductile shear zones in the Caledonides of northern Sweden: a three-dimensional puzzle. *Journal of Structural Geology*, 23, 1549–1565. DOI: 10.1016/S0191-8141(01)00020-7
- Flinn, D.: 1962, On folding during three-dimensional progressive deformation. *Quarterly Journal of the Geological Society*, 118, 385–428. DOI: 10.1144/gsjgs.118.1.0385
- Fossen, H.: 2016, *Structural geology*, Cambridge University Press.
- Fossen, H. and Cavalcante, G.C.G.: 2017, Shear zones—A review. *Earth-Science Reviews*, 171, 434–455. DOI: 10.1016/j.earscirev.2017.05.002
- Francois, T., Agard, P., Bernet, B., Meyer, B., Chung, S.-L., Zarrinkoub, M.H., Burov, E. and Monie, P.: 2014, Cenozoic exhumation of the internal Zagros: first constraints from low-temperature thermochronology and implications for the build-up of the Iranian plateau. *Lithos*, 206–207, 100–112. DOI: 10.1016/j.lithos.2014.07.021
- Ghasemi, A. and Talbot, C.J.: 2006, A new tectonic scenario for the Sanandaj–Sirjan Zone (Iran). *Journal of Asian Earth Sciences*, 26, 683–693. DOI: 10.1016/j.jseas.2005.01.003
- Heidari, S., Rastad, E., Mohajjel, M. and Shamsa, M.: 2006, Gold mineralization in ductile shear zone of Kervian (southwest of Saqez-Kordestan province). *Geosciences*, 58, 18–37, (only English abstract).
- Jackson, J.: 1992, Partitioning of strike-slip and convergent motion between Eurasia and Arabia in eastern Turkey and the Caucasus. *Journal of Geophysical Research: Solid Earth*, 97, 12471–12479. DOI: 10.1029/92JB00944

- Liang, C., Liu, Y., Neubauer, F., Bernroider, M., Jin, W., Li, W., Zeng, Z., Wen, Q. and Zhao, Y.: 2015, Structures, kinematic analysis, rheological parameters and temperature-pressure estimate of the Mesozoic Xingcheng-Taili ductile shear zone in the North China Craton. *Journal of Structural Geology*, 78, 27–51. DOI: 10.1016/j.jsg.2015.06.007
- Mohajjel, M., Fergusson, C. and Sahandi, M.: 2003, Cretaceous–Tertiary convergence and continental collision, Sanandaj–Sirjan zone, western Iran. *Journal of Asian Earth Sciences*, 21, 397–412. DOI: 10.1016/S1367-9120(02)00035-4
- Mohajjel, M. and Fergusson, C.L.: 2000, Dextral transpression in Late Cretaceous continental collision, Sanandaj–Sirjan zone, western Iran. *Journal of structural geology*, 22, 1125–1139. DOI: 10.1016/S0191-8141(00)00023-7
- Mohajjel, M. and Rasouli, A.: 2014, Structural evidence for superposition of transtension on transpression in the Zagros collision zone: Main recent fault, Piranshahr area, NW Iran. *Journal of Structural Geology*, 62, 65–79. DOI: 10.1016/j.jsg.2014.01.006
- Montesi, L.G.: 2013, Fabric development as the key for forming ductile shear zones and enabling plate tectonics. *Journal of Structural Geology*, 50, 254–266. DOI: 10.1016/j.jsg.2012.12.011
- Mookerjee, M. and Fortescue, F.Q.: 2016, Quantifying thinning and extrusion associated with an oblique subduction zone: An example from the Rosy Finch Shear Zone. *Tectonophysics*, 693, 290–303. DOI: 10.1016/j.tecto.2016.06.012
- Mookerjee, M. and Nickleach, S.: 2011, Three-dimensional strain analysis using Mathematica. *Journal of Structural Geology*, 33, 1467–1476. DOI: 10.1016/j.jsg.2011.08.003
- Mookerjee, M. and Peek, S.: 2014, Evaluating the effectiveness of Flinn's k-value versus Lode's ratio. *Journal of Structural Geology*, 68, 33–43. DOI: 10.1016/j.jsg.2014.08.008
- Mouthereau, F., Lacombe, O. and Verges, J.: 2012, Building the Zagros collisional orogen: timing, strain distribution and the dynamics of Arabia/Eurasia plate convergence. *Tectonophysics*, 532, 27–60. DOI: 10.1016/j.tecto.2012.01.022
- Mulchrone, K.F. and Talbot, C.J.: 2014, Constraining the strain ellipsoid and deformation parameters using deformed single layers: A computational approach assuming pure shear and isotropic volume change. *Journal of Structural Geology*, 62, 194–206. DOI: 10.1016/j.jsg.2014.02.002
- Passchier, C.W. and Trouw, R.A.: 2005, *Microtectonics*, Springer Science and Business Media.
- Ramsay, J.: 1980, Shear zone geometry: a review. *Journal of structural geology*, 2, 83–99. DOI: 10.1016/0191-8141(80)90038-3
- Ramsay, J. and Allison, I.: 1979, Structural analysis of shear zones in an alpinised Hercynian granite (Maggia Lappen, Pennine Zone, Central Alps). *Schweizerische mineralogische und petrographische Mitteilungen*, 59, 251–279.
- Ramsay, J. and Graham, R.: 1970, Strain variation in shear belts. *Canadian Journal of Earth Sciences*, 7, 786–813. DOI: 10.1139/e70-078
- Sarkarinejad, K., Samani, B., Faghih, A., Grasemann, B. and Moradipoor, M.: 2010, Implications of strain and vorticity of flow analyses to interpret the kinematics of an oblique convergence event (Zagros Mountains, Iran). *Journal of Asian Earth Sciences*, 38, 34–43. DOI: 10.1016/j.jseas.2009.12.015
- Şengör, A. and Kidd, W.: 1979, Post-collisional tectonics of the Turkish-Iranian plateau and a comparison with Tibet. *Tectonophysics*, 55, 361–376.
- Shan, Y.: 2008, An analytical approach for determining strain ellipsoids from measurements on planar surfaces. *Journal of Structural Geology*, 30, 539–546. DOI: 10.1016/j.jsg.2006.12.004
- Sheikholeslami, M.: 2015, Deformations of Palaeozoic and Mesozoic rocks in southern Sirjan, Sanandaj–Sirjan Zone, Iran. *Journal of Asian Earth Sciences*, 106, 130–149.
- Simpson, N.C.: 1981, Ductile shear zones: a mechanism of rock deformation in the Orthogneisses of the Maggia Nappe Ticino. *Geologisches Institut der Eidgenössische Technischen Hochschule und der Universität Zürich*
- Soares, A. and Dias, R.: 2015, Fry and Rf/φ strain methods constraints and fold transection mechanisms in the NW Iberian Variscides. *Journal of Structural Geology*, 79, 19–30. DOI: 10.1016/j.jsg.2015.07.005
- Talebian, M. and Jackson, J.: 2002, Offset on the main recent fault of NW Iran and implications for the late Cenozoic tectonics of the Arabia–Eurasia collision zone. *Geophysical Journal International*, 150, 422–439. DOI: 10.1046/j.1365-246X.2002.01711.x
- Toy, V. G., Prior, D. J., Norris, R. J., Cooper, A.F. and Walrond, M.: 2012, Relationships between kinematic indicators and strain during syn-deformational exhumation of an oblique slip, transpressive, plate boundary shear zone: the Alpine Fault, New Zealand. *Earth and Planetary Science Letters*, 333, 282–292. DOI: 10.1016/j.epsl.2012.04.037
- Watts, M. and Williams, G.: 1983, Strain geometry, microstructure and mineral chemistry in metagabbro shear zones: a study of softening mechanisms during progressive mylonitization. *Journal of Structural Geology*, 5, 507–517. DOI: 10.1016/0191-8141(83)90056-1
- Zhang, B., Zhang, J. and Zhong, D.: 2010, Structure, kinematics and ages of transpression during strain-partitioning in the Chongshan shear zone, western Yunnan, China. *Journal of Structural Geology*, 32, 445–463. DOI: 10.1016/j.jsg.2010.02.001
- Zhang, Z., Xiao, W., Ji, W., Majidifard, M.R., Rezaeian, N.M., Talebia, M., Xiang, D., Chen, L., Wan, B. and Ao, S.: 2018, Geochemistry, zircon U-Pb and Hf isotope for granitoids, NW Sanandaj–Sirjan zone, Iran: Implications for Mesozoic–Cenozoic episodic magmatism during Neo-Tethyan lithospheric subduction. *Gondwana Research*, 62, 227–245. DOI: 10.1016/j.gr.2018.04.002